



Versatile bioactive and antibacterial coating system based on silica, gentamicin, and chitosan: Improving early stage performance of titanium implants



J. Ballarre^{a,b,*}, T. Aydemir^a, L. Liverani^a, J.A. Roether^c, W.H. Goldmann^d, A.R. Boccaccini^{a,**}

^a Institute of Biomaterials, University Erlangen-Nuremberg, Cauerstrasse 6, 91058 Erlangen, Germany

^b Material's Science and Technology Research Institute (INTEMA), UNMdP-CONICET, Av. Colón 10850, Mar del Plata 7600, Argentina

^c Institute of Polymer Materials, University Erlangen-Nuremberg, 91058 Erlangen, Germany

^d Department of Physics, Biophysics Group, University Erlangen-Nuremberg, 91052 Erlangen, Germany

ARTICLE INFO

Keywords:

Bioactive glass
Titanium
Silica-gentamicin nanoparticles
Electrophoretic deposition
Bioactivity
Antibacterial effect

ABSTRACT

The aim of this work is to develop and characterize a multifunctional and dual surface coating system for titanium orthopedic implants by applying two different cost-effective, scalable, and non-complex coating technologies (spray and electrophoretic deposition). The first deposit is formed by a sprayed hybrid sol-gel layer combined with bioactive glass particles (45S5, BG), and the outer part of the dual coating consists of a chitosan-gelatin/silica (Si) - antibiotic (gentamicin, Ge) composite layer applied by electrophoretic deposition. The application of sol-gel enclosed BG drops onto the surface was done to enhance the bioactivity of the double-layered surface coating system. After the BG is dissolved, thus generating a calcium-silicon rich medium, the re-deposition of hydroxyl-carbonate apatite occurs. Regarding the antibacterial inhibition properties, antibacterial activity to both strains used (*S. aureus* and *E. coli*) was obtained for the chitosan/gelatin/Si-Ge nanoparticle coatings on titanium substrates, showing a large inhibition area around the samples. Both the bare Ti samples and the coatings with chitosan/gelatin matrix did not successfully inhibit bacterial growth. As expected, the presence of silica-based glasses and coatings based on amorphous silica enhanced cell viability. The deposition of BG was done with the aim of extending the bioactive effect of the system, considering the presence of a porous degradable organic layer deposited on top, which was shown to be partially degraded after 7 days. The sol gel sprayed BG layer combined with chitosan/gelatin biopolymers filled with Si-Ge nanoparticles presents a suitable technology to generate bioactive and antibacterial surfaces to enhance Ti implant performance.

1. Introduction

Stainless steel, titanium alloys, and cobalt-chrome alloys are the preferred metals for permanent implants in orthopedic surgery since they have excellent characteristics such as corrosion resistance, mechanical stability, fracture toughness as well as biocompatibility [1,2]. However, with the current innovations in medical technology and the resulting increased life expectancy, there is a high demand for research on alternative multi-functional biomaterials for implants [3]. The main goal and the most important challenges of current research are to extend the lifetime of implants and eliminate problems that may limit their life time, for example severe complications such as loosening or

implant-associated infections, which cannot be completely avoided or prevented [4–6]. Such impairments lead to serious health consequences, e.g. subsequent surgical operations for the removal and/or the revision of implants, which can in turn lead to new problems and seriously compromise the quality of life of the patients representing an unsatisfactory and expensive situation with negative socio-economic impact.

Compared to stainless steel 316L, titanium alloys generally proved a better tolerance for stress loading and fatigue [6]. As a reactive metal, titanium is able to form a dense and stable oxide layer on its surface, which provides biocompatibility and high resistance against corrosion. Further, titanium is generally characterized by low thermal expansion

* Correspondence to: J. Ballarre, Material's Science and Technology Research Institute (INTEMA), UNMdP-CONICET, Av. Colon 10850, 7600 Mar del Plata, Argentina.

** Correspondence to: A.R. Boccaccini, Institute of Biomaterials, Department of Materials Science and Engineering, University of Erlangen-Nuremberg, Cauerstraße 6, 91058 Erlangen, Germany.

E-mail addresses: jballarre@fi.mdp.edu.ar (J. Ballarre), aldo.boccaccini@ww.uni-erlangen.de (A.R. Boccaccini).

<https://doi.org/10.1016/j.surfcoat.2019.125138>

Received 1 October 2019; Received in revised form 30 October 2019; Accepted 4 November 2019

Available online 05 November 2019

0257-8972/ © 2019 Elsevier B.V. All rights reserved.

and low weight [7]. In contrast to stainless steel 316L, the Young's modulus of titanium (100–115 GPa) is more comparable with the one of native bone, which reduces stress shielding effects [8,9].

Cemented and cementless prostheses are used in orthopedic surgery and their relative advantages and drawbacks have been discussed based on their relative cost, complexity of the surgical procedure, and post-operative quality of life among others [10,11]. In this context, a second challenge appears: the need to modify the implant surface to enhance the osseointegration process when cement-less implants are used, which should ultimately improve bone fixation and stabilization. Significant research efforts have been made to optimize the bone implant interface to accelerate bone healing and to improve bone anchorage; coating of metallic implants by bioactive layers represents one of the proposed approaches [12,13].

Organic-inorganic hybrid sol-gel-based materials have attracted the attention from researchers in academy and industry due to the unusual and favorable combination of their chemical and physical properties [14,15]. Hybrids with the greatest potential for industrial applications are derived from hydrolytic condensation products of functionalized alkoxy silanes, pure or enriched with tetraethoxysilane (TEOS) [16,17]. For example, the final hybrid material consists of a slightly modified Si-O-Si network with methyl- or ethyl-organic groups.

The spray-coating technology is a widely used method for several surface deposition processes [18]. Generally, the process is based on aerodynamics and speed impact dynamics. Sprayed particles are accelerated at high velocity by a gas flow, reaching the substrate surface and forming a coating due to impact deformations. This technique is utilized, for example, for wear or fatigue resistance coatings, aesthetic coatings, barrier or protective coatings, and sealing coatings [19,20]. Moreover, spray deposition is also used for biomedical surface modifications by the addition of various functionalizing materials [21,22]. In addition, it has several advantageous features, such as enabling control over coating thickness, providing a homogeneous, continuous, and crack-free layer, allowing an easy application on large areas, even on complex geometries.

Even though a hybrid sol-gel coating can improve corrosive behavior of metallic substrates, osseointegration cannot take place on surfaces, which are not bioactive (*i.e.* exhibiting bone bonding ability), and therefore another strategy is required to induce strong bonding to bone tissue. Biomaterials, and specially bioceramics, have been developed and modified from being inert to bioactive [23]. Silicate glasses (bioactive glasses) as materials for bone bonding were presented for the first time by Hench in the late 1960s [24]. The first composition that was confirmed to establish strong bonds to bone was labeled as 45S5 due to its silica content (45% wt.) [25]. As bioactive glasses (or glass-ceramics) have the ability to bond with living tissues forming an apatite layer, they represent an attractive group of materials for the development of coatings on metallic implants for dental and orthopedic applications [26].

To avoid bacterial colonization, the use of several antibacterial agents incorporated to coatings has been studied widely [27–32]. A commonly used antibiotic is gentamicin, suitable to prevent implant-related infections in a short time after surgery. The use of antibiotics is controversial, since concentrations below the minimum inhibitory concentration (MIC) for each species could generate antibiotic resistance [33].

Since silica-based nanomaterials and their synthesis processes are biocompatible, cost effective, easily to handle as well as scalable for industrial purposes, they are good candidates for developing functional coatings [34]. Depending on size and dose, they are also catalogued as hydrophilic and non-toxic [35]. A further feature is that the degradation product (silicic acid) beneficially supports the formation of connective tissues [32]. In the typical nanoparticle shape (spherical), silica is investigated as a promising carrier system for drug delivery [36]. One suggested use of this drug delivery system was presented by Wang et al. [32], who reported the incorporation of gentamicin sulfate during the

silica nanoparticle preparation for the development of an antibacterial carrier for preventing infections in bone or dental implants.

Electrophoretic deposition (EPD) is a versatile processing method suitable to produce coatings at room temperature, allowing the processing of a broad spectrum of materials [37]. Fine powder or colloidal suspensions of different materials including metals, polymers, ceramics, glasses, and their composites can be deposited by EPD. By combining electrophoresis and deposition, this technique offers many advantages, being favorable for diverse bioactive coating systems [38,39]. EPD facilitates producing uniform, stable, mechanically resistant coatings of variable thickness on different shaped substrates as well as on three-dimensional complex and porous structures [40–42]. Many substances and materials can be used for electrophoretic deposition of coatings for orthopedic applications. Most of them include chitosan and/or gelatin coating matrices, which were modified or enhanced differently to obtain various coating features [39,43–47]. Chitosan, which is mainly obtained by alkaline *N*-deacetylation of shrimp and crab shell chitin on an industrial scale, is chemically stable, biocompatible, has good mechanical properties, promotes cell adhesion, and has good film-forming properties [48]. Another important natural biopolymer is gelatin, which finds application in a wide range of fields, for example, in the medical, pharmaceutical, as well as food industry.

The aim of this work is to develop and characterize a multi-functional and dual surface coating system for titanium orthopedic implants by applying two different cost-effective, scalable, and non-complex coating technologies, namely spray deposition and electrophoretic deposition. In this coating system, the first deposition layer represents a sprayed hybrid sol-gel layer combined with bioactive glass particles (45S5 BG), whereas the outer part of the dual coating consists of a biopolymer/silica-antibiotic (gentamicin) composite layer applied by EPD.

2. Materials and methods

2.1. Substrate and sprayed first coating

Rectangular specimens of 0.3 mm (thickness) × 25 mm × 15 mm of commercially pure titanium (cpTi grade 2, ANKURO, Germany) were used. The samples were polished with 600, 1000, and 1200 grit paper and washed with isopropyl alcohol (VWR, Germany).

A first coating was applied to bare surfaces by the spray technique. A sol-gel silica-based coating (TM) with 10% in weight of commercially available BG particles (45 s5 composition, Vitryxx®, Schott) of 4 μm mean particle size, was applied to create bioactive anchorage points on the surface. The hybrid organic-inorganic sol to produce the TM coating was prepared with tetraethoxysilane (TEOS, 99% Sigma Aldrich), and methyltriethoxysilane (MTES, 98% Sigma Aldrich). The molar ratio of the alkoxide was kept constant (TEOS/MTES = 40/60). The final silica concentration was 180 g/L, and the amount of water was kept at a stoichiometric ratio. The synthesis was performed by acidic catalysis with nitric acid (65% w/w, Sigma). The suspension of the particles was generated by vigorous stirring and immersion in an ultrasonic bath for 20 min.

The first layer of the dual surface coating system was realized by using a double-action-trigger-type spray gun (Iwata neo TRN 2, ANEST IWATA). For the deposition, the spray gun was connected to a compressed air source at a pressure of 3 bar through the nozzle; the substrates were fixed at a height of 23 cm and their distance to the spray gun nozzle was 20 cm. While the flow rate (\dot{V}) of the bioactive mixture was determined as 19.5 $\frac{\text{ml}}{\text{s}}$, a double spray pass along the lateral movement axis was chosen. With the impact of the sol-encased BG particles on the substrate surface, a dropwise spread deposit was developed. Finally, the coatings were sintered at a temperature of 450 °C for 30 min.

Further, commercial titanium screws (grade 2, Carper Mecanizados,

Tandil SA, Argentina) of 15 mm length and 2 mm diameter were coated. While the substrate was fixed centrally on the rotation element at a height of 20 cm, its rotating speed was determined as $0.028 \frac{m}{s}$. With a flow rate \dot{V} of $19.5 \frac{ml}{s}$, the screw was sprinkled with the bioactive mixture (hybrid sol/Bioglass® composite) during 7 rotation cycles at 3 bar operation pressure. The distance between the gun's nozzle and target was set as 20 cm.

2.2. Synthesis of Silica-Gentamicin (Si-Ge) nanoparticles

The synthesis of gentamicin-loaded silica nanoparticles is based on the Stöber method. According to Wang et al. [32], 75 mL ethanol (VWR International, 96%, Germany) was used together with 3.4 mL ammonia solution (EMPROVE® Merck KGaA, 25%, Germany) for dissolving 20 mg gentamicin sulfate powder (Sigma Aldrich) under magnetic stirring. Subsequently, 0.2 mL of tetraethoxysilane (TEOS, Sigma Aldrich® 99%, Germany) was dropped into the solution during vigorous stirring. After 1 h, the stirring rate was lowered, and the mixture was stirred at room temperature for another 24 h. Afterwards, the solution was washed with distilled water four times, and centrifuged (6000 rpm, at room temperature for 10 min). The supernatant was removed after centrifugation. The powder product was finally obtained by freeze-drying (Freeze Dryer Alpha 2-4 LSC plus, Christ, Germany). This controlled experimental process enabled the incorporation of drug molecules into silica nanoparticles during their growth [36].

2.3. Chitosan/gelatin/Si-Ge nanoparticles coatings by electrophoretic deposition (EPD)

For EPD processes, a colloidal polyelectrolyte complex of chitosan and gelatin was synthesized. Medium molecular weight chitosan (deacetylation degree of 75–85%, Sigma Aldrich, Germany) was used. The complete dissolution of 0.05 g of chitosan in 20 mL de-ionised water and 1 mL acetic acid (PROLABO® VWR International, 99–100%) was achieved by magnetic stirring after 30 min. Then, to reduce adverse hydrogen formation during EPD, which affects the homogeneity of the coating [49], ethanol (EMSURE® Merck KGaA, 99% purity) was added to reach a final concentration of 79% (v/v) and stirred at room temperature for 24 h. The final chitosan solution (pH = 4) was stored in the fridge at 4 °C. To obtain a gelatin solution, 0.1 g of gelatin type B (Sigma Aldrich, Germany) was mixed into 20 mL of de-ionised water and 1 mL of acetic acid at 45 °C for 1 h. After cooling down to room temperature, 79 mL of ethanol was added to the mixture. The completed suspension (pH = 4) was stirred for another 20 min and then placed at 4 °C for storage.

The separately prepared solutions of the biopolymers (chitosan and gelatin) were mixed in equal amounts (1:1 ratio) using magnetic stirring for 10 min. This resulted in a composition of 33 wt% chitosan and 67 wt% gelatin. After the mixture was completed, 2 g/L of gentamicin loaded-silica nanoparticles (Si-Ge nanoparticles) were added to the solution.

All EPD coatings were obtained by applying a direct current (DC) with an EX735M Multi-Mode PSU 75V/150V 300W power supply (Thurlby Thandar Instruments Ltd., Germany). As the deposition substrate, spray-coated Ti sheets were used. Planar sheets of AISI 316L stainless steel plates (ThyssenKrupp AG, Germany) were used as counter electrodes. Prior to the deposition process, the electrodes were cleaned with isopropyl alcohol in an ultrasonic bath for 10 min. The electrodes were installed vertically in parallel configuration and the distance adjusted by 10 mm. The volume of the EPD cells was 40 mL. The deposition process was conducted by applying a constant voltage of 15V for 3 min at room temperature. After the coating process, the samples were air-dried and stored in desiccators.

For coating the screw samples, they were positioned in the center of a cylindrical 316L stainless steel counter electrode with a diameter of

1.4 mm (formed out of a 0.3×15 mm coil ISO 9445-1, ThyssenKrupp AG). A conductive copper wire was used for the correct height adjustment of the cathode by wrapping it around the screw shaft. It also enabled the ongoing flow of electricity and induced the coatings process. The distance between electrodes was 0.6 cm and the voltage applied was 15V for 3 min.

2.4. In vitro bioactivity characterization

Before the *in vitro* characterization tests of the coated samples were performed, the adhesion of the systems was measured by the ASTM D3359- B method. Therefore, on each coating surface down to the substrate, a lattice pattern with two orthogonal cuts was made by using a cross-hatch cutter (Model Elcometer 107). After the application of an adhesive tape, it was peeled off manually at an angle of 60° to the substrate surface. For assessment of the detachment's level a comparison with the standard ASTM chart was accomplished. The visual results were recorded by utilizing the M50 microscope (Leica).

The coated samples were analyzed *in vitro* by immersion in a solution that simulates the inorganic concentration of ions in human blood plasma. The objective is to detect the possible formation of hydroxyapatite and to evaluate the degradation of the coatings [50]. Simulated body fluid (SBF) solution was used as electrolyte in all the experiments. SBF was prepared with the following chemical composition [51,52]: NaCl ($8.053 \text{ g}\cdot\text{L}^{-1}$), KCl ($0.224 \text{ g}\cdot\text{L}^{-1}$), CaCl₂ ($0.278 \text{ g}\cdot\text{L}^{-1}$), MgCl₂·6H₂O ($0.305 \text{ g}\cdot\text{L}^{-1}$), K₂HPO₄ ($0.174 \text{ g}\cdot\text{L}^{-1}$), NaHCO₃ ($0.353 \text{ g}\cdot\text{L}^{-1}$), and (CH₂OH)₃ CNH₂ ($6.057 \text{ g}\cdot\text{L}^{-1}$). 1 M HCl was added to adjust the pH to 7.25 ± 0.05 . The samples were immersed in SBF for 1, 3, and 7 days, and sealed at 37 °C in a sterilized shaking incubator for the determined time period.

In order to analyze *in vitro* bioactivity, Fourier Transformed Infrared spectroscopy (FTIR) and X Ray Diffraction (XRD) tests were conducted on previously immersed samples in SBF. FTIR (Shimadzu IRAffinity-1S, Shimadzu Corp.) was used in order to analyze the chemical structure and bonding of coatings. All data were obtained in transmittance mode using 32 scans at a wavenumber in the range of $400\text{--}4000 \text{ cm}^{-1}$ and a resolution of 4 cm^{-1} . For identifying crystallographic structures, an X-Ray diffractometer (MiniFlex 600, Rigaku) was used with Cu-K α radiation at 40 kV and 15 mA. To eliminate the metal background, a XRD pattern was obtained for each coating by scratching off. Measurements were performed at standard conditions, applying a 2theta range from 20° to 50°, a step size of 0.02°, and a count rate of 4° per minute. Scanning Electron Microscopy (Auriga ZEISS SNr. 4570, Carl Zeiss Microscopy) with 1 keV electric beam power was used to investigate the surface of the coated samples before and after SBF tests.

2.5. In vitro gentamicin release

The release of gentamicin from multi-component depositions for both coating systems was defined and analyzed using an UV-VIS Spectrometer (Specord40 by Analytik Jena). Employing the software WinASPECT 2.5.8.0, the characteristic absorption peak for gentamicin was detected at a wavelength of 400 nm. The UV/VIS spectrum of all samples was measured between 300 and 700 nm in disposable cuvettes. Every 0.5 nm, a measuring point was recorded at a speed of $10 \frac{nm}{s}$.

Gentamicin capability to absorb visible/ultraviolet light is limited. In order to develop a notable peak of gentamicin, ninhydrin was used in this experimental part as a derivatizing agent. Ninhydrin is a reagent, which is usually utilized for qualitative identification of drugs containing amino groups [53]. To prepare the ninhydrin stock-solution, 10 mg of solid ninhydrin (Sigma Aldrich™, Germany) was dissolved in 5 mL phosphate buffered saline (PBS) solution. The measurement was carried out against a PBS-ninhydrin mixture as reference.

A calibration curve was created for calculating the individually released concentrations from each sample. For the measurement of the

drug release, each coating condition was carried out in triplicate in 5 mL of PBS (Sigma Aldrich™) and was incubated at 37 °C for 30 min, 1 h, 2 h, 4 h, 8 h, 24 h, 48 h, 5 days, 8 days, 14 days, and 21 days. At each time-point, 1 mL of the sample solution was removed for analysis, while the same amount was replaced by fresh PBS. 0.3 mL of a ninhydrin stock-solution was added to the aliquot and heated up to 95 °C in a water bath for 15 min. After cooling down, the spectrometric scan was performed. The samples were done in triplicate.

2.6. Antibacterial tests

Gram-positive *Staphylococcus aureus* and Gram-negative *Escherichia coli* were used. The stock suspension of bacteria was prepared by suspending a certain amount of known bacteria in 10 mL of sterile LB medium (Luria/Miller medium, Carl Roth, Germany) and growing the bacteria overnight in a shaker at 37 °C. The suspension was used and diluted for each experiment to reach a concentration of bacteria of 0.015 at OD 600 nm (OD, optical density) measured in a spectrophotometer Biophotometer Plus, (Eppendorf AG).

2.6.1. Halo inhibition tests

Antibacterial agar diffusion assays were carried out as follows: 20 µL of the prepared suspension was deposited and spread homogeneously onto an agar (LB Agar (Lennox) Lab M Ltd.) petri dish. The samples were placed onto the surface of the agar plates, and the culture was incubated for 24 h at 37 °C. After the incubation time, the inhibition zone around each sample was documented by a digital camera.

2.6.2. Turbidity measurements or antibacterial suspension effect

For turbidity measurements, each sample was analyzed in triplicate. The sterilized samples (1 h under UV light) were placed in 24 multi-well plates and filled with 2 mL of LB-medium and the corresponding amount of bacteria required reaching 0.015 OD 600 nm in each well plate as explained above. The samples with the bacteria were incubated at 37 °C. At given time-points (3, 6, 8, 24, 30, and 48 h) aliquots of bacterial suspension of each well plate were withdrawn, and the variation in optical density was measured.

2.7. Cell attachment and proliferation

Bone marrow-derived murine stromal cells (ST-2 cell line) (Leibniz-Institute DSMZ – German Collection of Microorganisms and Cell Cultures GmbH, Germany) were used to assess cell viability and morphology on the substrate. All samples were placed in sterile 12 multi-well plates and exposed to UV light for 1 h.

ST-2 cells were cultured in RPMI 1640 medium (Thermo Fisher Scientific), supplemented with 10% fetal bovine serum (Lonza) and 1% penicillin/streptomycin (Lonza) and incubated at 37 °C and 5% CO₂. The seeding on the substrate was performed by adding a drop of 100 µL of cell suspension at an inoculum ratio of 1.5×10^5 cells/mL in the center of the substrate, to avoid cell adhesion below the samples. The samples were put in the incubator for 15 min after the deposition of the drop, then 2 mL of RPMI medium was added to each well. To assess cell viability, after 1 day and 7 days of seeding, the WST-8 assay ((2-(2-methoxy-4-nitrophenyl)-3-(4-nitrophenyl)-5-(2,4-disulphophenyl)-2H-tetrazolium, monosodium salt), Sigma Aldrich, Germany) was performed.

Fluorescence microscopy and SEM analysis were used to investigate the morphology of the adherent cells on the substrate. The dyes, rhodamine phalloidin and DAPI, (ThermoFisher Scientific) were used for the staining of actin filaments and cell nuclei, respectively. The protocol for staining contains an initial step of immersion of the samples in a fixation solution containing 1,4-piperazinediethanesulfonic acid buffer, ethylene glycol tetra-acetic acid, polyethylene glycol, paraformaldehyde, PBS, and sodium hydroxide (Sigma) and permeabilization buffer, containing triton X-100, sucrose and PBS (Sigma Aldrich).

Subsequently, rhodamine phalloidin and DAPI were added at concentrations of 8 µL/mL and 1 µL/mL to each well, respectively. Fluorescence microscopy (Axio Scope A1, Zeiss) was used for the analysis. For SEM analysis, the samples were fixed using fixation solutions containing glutaraldehyde, paraformaldehyde, sucrose, and sodium cacodylate trihydrate (Sigma Aldrich, Germany); after the graded ethanol series, the samples were sputtered with gold (Sputter Coater Q150T, Quorum Technologies) and analyzed by SEM (Auriga ZEISS SNr. 4570, Carl Zeiss Microscopy).

3. Results and discussion

3.1. Coating morphology

The spray coating technique is a versatile one that can be used for non-conductive suspensions and substrates, but it has some disadvantages as the viscosity of the flow, the fillers of the solution, and the difficulties to adapt the coating procedure to really complex figures. EPD, in contrast, is a suitable technique for coating complex shapes due to the applied electric field acting between the suspension and the target. In a suspension of charged colloidal particles and with a conductive substrate as deposition electrode, the current lines are homogeneous, and the colloids are attracted to the surface where they deposit. The aim to use both techniques is to obtain well-dispersed and attached bioactive points (BG-sol gel sprayed first layer) and then to cover the complete surface of the sample with a bioactive and antibacterial layer, obtained by EPD.

As illustrated in Fig. 1, the sprayed, commercially pure titanium substrates (from now on named as Ti) display a dropwise randomly spread deposit of the sol-gel/BG solution (from now on named Ti-BG). The area covered by bioactive glass particles was 5% (calculated by the software Image J) [54]. The rest of the non-coated surfaces of the Ti samples provides thus adequate electric conductivity for the subsequent EPD coating step.

The coatings with chitosan and gelatin without Si–Ge nanoparticles (from now on named Ti-BG-EPD) presented a relatively smooth and uniform structure. From Fig. 2, the “nano” characteristic of the Si–Ge particles are visible, which exhibit an average diameter of 200 nm. When the composite coating is applied, the obtained surface shows many differently shaped particles that are distributed over the entire surface. At high magnifications, the chitosan and gelatin film with Si–Ge nanoparticles (from now on Ti-BG-EPD SiGe) denotes agglomeration in some areas; but it can be observed that nanoparticles are distributed over the complete surface of the coating (Fig. 2).

Through intermolecular interactions between the polyelectrolyte complex of chitosan and gelatin (PEC) and the particles, a stable colloidal complex is formed. Silica nanoparticles in colloidal solutions are negatively charged at the pH value of 4 [55]. Both, repulsive and attractive interactions between molecules and charges of chitosan and gelatine cannot be avoided [37,55–57]. According to Patel et al. [46], these kinds of interactions between negatively charged components and the chitosan/gelatin PEC are strong enough to allow particles to be carried along with the PEC during the deposition procedure, because of their high mobility. Agglomeration within a colloidal suspension leads to particle sedimentation and provides instability. Moreover, high viscosity prevents particle mobility due to strong interactions and impairs as a result the suspension stability as well [58].

The estimated thickness measurement of the dual coatings was performed by Scanning Electron Microscopy (SEM), see Fig. 2 (right). The chitosan and gelatin EPD coatings on CP-Ti substrate possess a thickness of 5.0 ± 0.7 µm and with the addition of silica-gentamicin nanoparticles the thickness increased to 12 ± 4 µm.

The surface roughness is one of the crucial features of biomaterials because it influences cell attachment and proliferation. The mean roughness was measured for all coatings in different conditions. Since titanium substrates were polished in a pre-treatment procedure, the

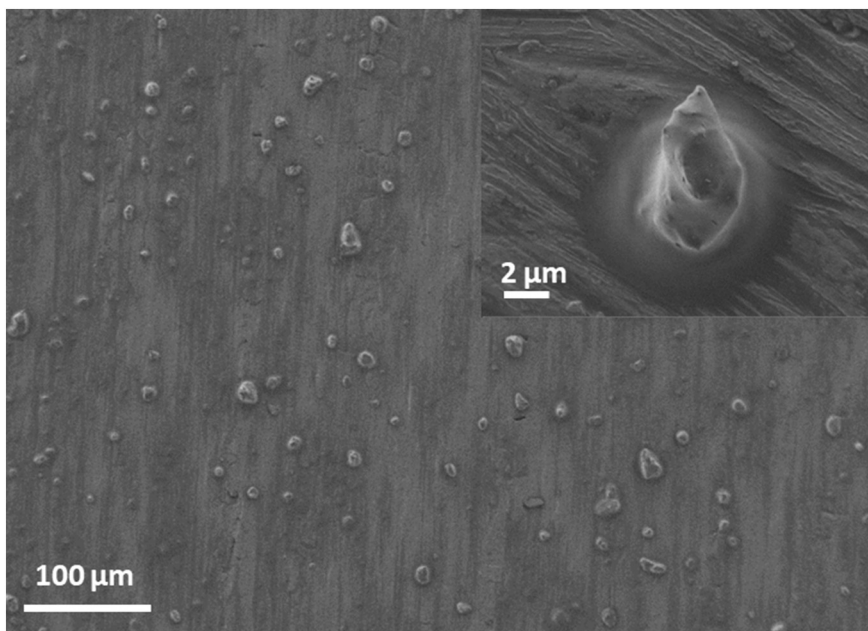


Fig. 1. SEM micrographs of CP-Ti spray-coated samples with 400× magnification and insert with 12,500×.

effect of parallel polishing lines on roughness was also examined employing transversal measurements. Table 1 shows the typical roughness parameters measured for the coatings and the bare CP-Ti substrate. Since the substrate has been polished, the direction of the roughness measurement could affect the results.

In both coating systems, the determined roughness values (R_a and R_z) correlate positively with the addition of synthesized silica particles. In comparison with bare substrates, a rapid increase of roughness values is clearly notable. Agglomerations of particles, already observed in morphological examinations, possibly promoted this increase of unevenness. The smooth and uniform chitosan/gelatin film was characterized by low roughness values. Indeed, the measured R_a and R_z variables for the double layer coating are even lower than those for the bare titanium substrate. These results indicate that the high roughness of bare titanium, which is caused by polishing, is significantly

decreased via covering with the biopolymer film, and a more uniform surface was provided.

The adhesion of the generated coatings was found to be almost perfect, between 4B and 5B following the ASTM standards. Fig. 3 shows the qualitative adhesion of the coatings after the test.

3.2. Wettability behavior

The wettability or contact angle of different biomaterials highly affects protein and cell attachment. On the one hand, according to Menzies and Jones [59], contact angles in the range 35°–80° are beneficial for the adhesion of osteoblasts. On the other hand, a contact angle of 55° is reported to provide optimal conditions for cell attachment and its growth [60]. Furthermore, Bumgardner et al. [61] reported that coatings based on chitosan are favorable for adhesion and

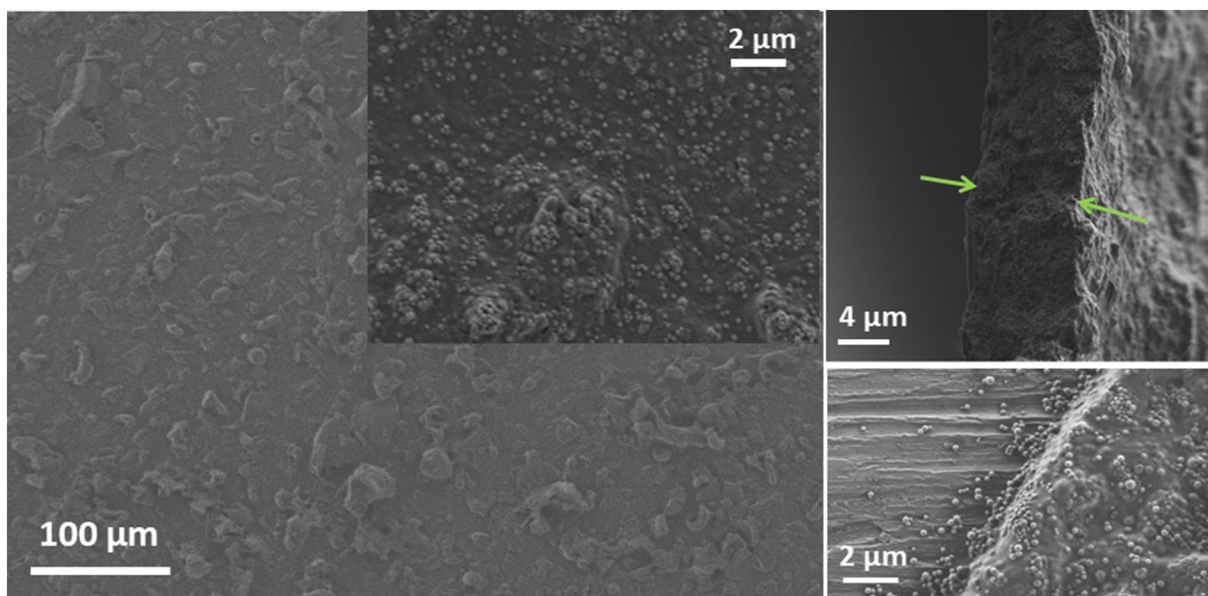


Fig. 2. Images of CP-Ti spray and EPD (chitosan/gelatin/SiGe) coated samples, generated by Scanning Electron Microscopy: (left) surface morphology; and (right) estimation of coatings thickness.

Table 1
Roughness results from double-layer titanium substrates.

CP-titanium grade 2					
Coating type	Layer number	Layer components	Direction of measurement	Ra [μm]	Rz [μm]
Bare substrate	0	–		0.42 ± 0.01	2.3 ± 0.1
Spray deposition	1	Bioactive sol		0.38 ± 0.0	2.04 ± 0.0
Spray deposition + EPD	2	Bioactive sol + chitosan/gelatin	transversal	0.45 ± 0.01	2.4 ± 0.1
			transversal	0.37 ± 0.02	1.5 ± 0.1
Spray deposition + EPD	2	Bioactive sol + chitosan/gelatin/SGN	transversal	0.32 ± 0.01	1.9 ± 0.2
			transversal	2.2 ± 0.4	9 ± 1
			transversal	1.7 ± 0.8	6 ± 1

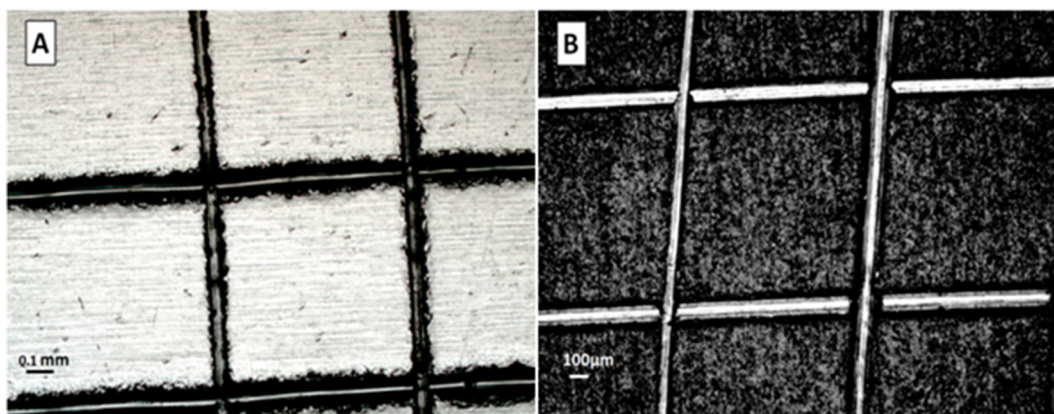


Fig. 3. Images of adhesion tape test following the ASTM 3359-B method with $5\times$ magnification (A) EPD chitosan and gelatin coating and (B) EPD of chitosan, gelatin and SiGe nanoparticles on cpTi- sol-gel drop BG substrates,

proliferation of osteoblasts, if the contact angle is around 60° .

Considering the results for the analyzed samples (Fig. 4), an increase in the measured angle of the different coatings is evident. Since bare titanium has a protective oxide layer on its surface, it is able to interact effectively with water molecules (hydrogen bridge bonding) and imparts a hydrophilic character to the surface. The sprayed layer consists of a sol containing bioactive particles, which is rich in silanols and induces hydrophilic properties. However, the total amount of the spray-deposited material (hybrid sol-gel and BG particles) is not enough to further enhance the hydrophilicity of the samples to a higher extent,

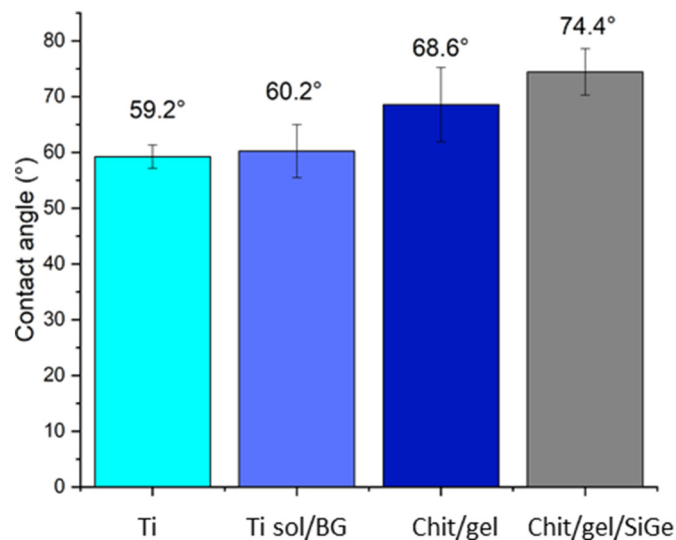


Fig. 4. Contact angle measurements with water drop test of the analyzed samples: bare Ti, Ti with sol-gel BG drops, EPD chitosan and gelatin coating and EPD chitosan/gelatin coating with SiGe nanoparticles.

compared to the bare substrate. The highest calculated contact angle for this coating system was found to be for the chitosan/gelatin/Si-Ge nanoparticle coatings and could be explained with the orientation of hydrophobic chain groups of both biopolymers on the surface: the incorporation of Si-Ge nanoparticles in the chitosan/gelatin matrix decreased the wettability of both coating systems. Nevertheless, the contact angles are within the desired range for optimal cell attachment and bone regeneration, reported to be around 55° as mentioned previously [60].

3.3. Coating bioactivity

The *in vitro* bioactive behavior of the coating systems was evaluated after immersion in SBF solution for different periods of time. SEM investigation carried out after treatment in SBF indicated an apparent slight degradation of the chitosan/gelatin matrix after 14 days of immersion. This result is acceptable, since gelatin is known for its fast degradation behavior at physiological temperature of 37°C [62]. Furthermore, in all coatings, needle-shaped apatite-like deposits were detected after 7 days of immersion. From these deposits, globular nuclei of “cauliflower-like” structure developed after 14 days of immersion in SBF (Fig. 5). The application of sol-gel enclosed BG drops onto the surface was done to enhance the bioactivity for the double-layered surface coating system of titanium. After the BG is dissolved, thus generating a calcium-silicon rich medium, the re-deposition of hydroxyl carbonate apatite (HCAp) occurs. However, a largely bare titanium surface area is present in the sprayed samples after immersion. Due to Ti-OH groups, the titanium surface becomes (at a physiological pH value of 7.4) negatively charged, which then leads to the attraction of Ca^{2+} ions from the SBF solution. Subsequently, the nucleation for apatite deposition is likely initiated by formed calcium titanates [63]. The present results show that, after the dissolution of the outer coating part, the lower layer may provide a prolonged bioactivity to the titanium substrates.

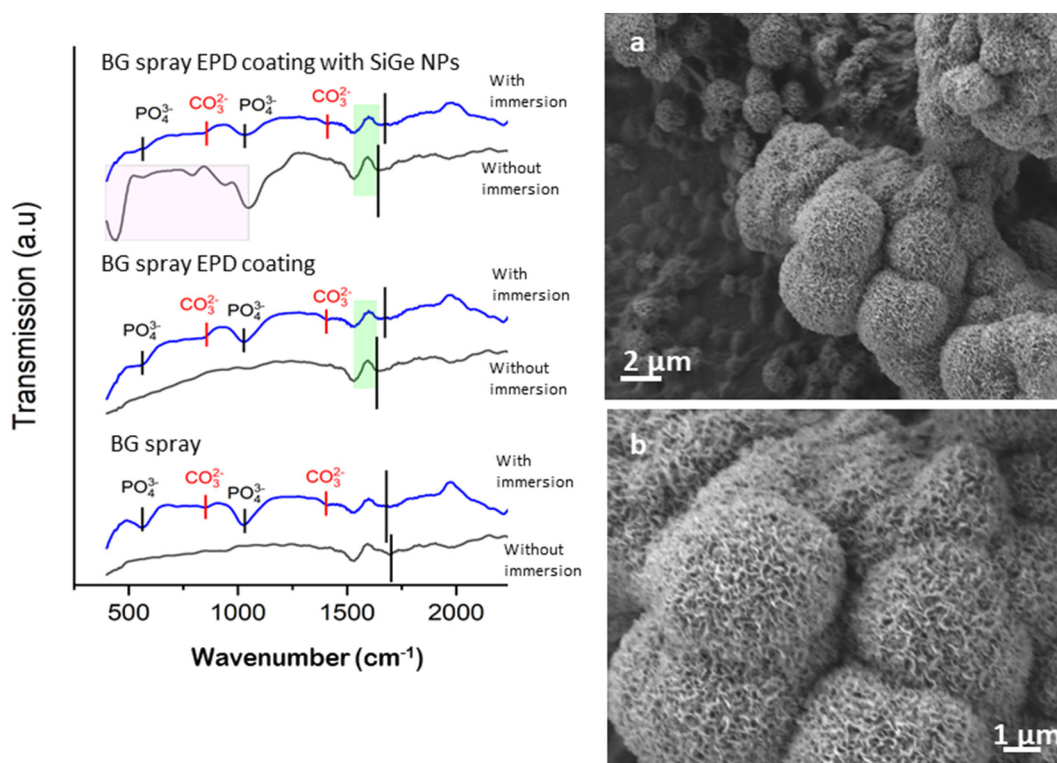


Fig. 5. (Left) FTIR spectra of dual coatings with titanium substrates before and after the SBF immersion for 14 days. (Right) SEM Images of CP-Ti sprayed EPD (chitosan/gelatin/SiGe NPs) coated samples after 14 days of immersion in SBF (a), 10,000 \times ; (b), 22,600 \times .

The degradation of the coatings and the presence of apatite-related compounds were analyzed with FTIR, and results are also shown in Fig. 5 (left). It is noticeable that the typical peaks of the main components (gelatin, chitosan, BG), as reported in literature, are present [64–66]. However, a minor shift to higher wavelength values can be observed in the range of amine and carbonyl groups of the chitosan/gelatin complex, which indicates the formation of new bonds or the adsorption of water [67]. Since silica is abundant in all coating types, the formation of calcium-phosphates is facilitated. The P–O stretching peak is present at 1030 cm^{-1} , and the P–O bending vibration is visible at 562 cm^{-1} . Furthermore, C–O bending and stretching peaks were detected at 852 cm^{-1} and 1410 cm^{-1} [68]. Therefore, it can be concluded that for this system the formation of HCAp has occurred after 14 days in SBF.

To confirm the presence of HCAp, XRD measurements were also performed. The results are referred to the immersion period of 14 days, and they are shown in Fig. 6. To eliminate the influence of the metal background, XRD patterns were obtained for each coating by detaching them from the substrate. Since the diffractogram was recorded for an interval of $2\theta = 20^\circ$ to 50° , chitosan and gelatin are not detected, since their peaks appear approximately at $2\theta = 10^\circ$ and $2\theta = 20^\circ$ [69]. In the analyzed coatings, characteristic peaks for HCAp around $2\theta = 23^\circ$ and $2\theta = 32.2^\circ$, $2\theta = 33.3^\circ$ and $2\theta = 26.4^\circ$ were observed. By the measured XRD patterns, it is apparent that all coatings show a high affinity to form HCAp upon immersion in SBF. Although degradation of the coatings was observed after 7 days of immersion, the residual coating areas are sufficiently large to induce the formation of HCAp at longer incubation times. This might be explained by the fact that the dual-coated system possess the first sprayed layer, which provides a prolonged bioactivity.

3.4. Antibacterial effect

As carriers for the antibacterial agent, silica nanoparticles were selected. Such nanoparticles are suitable to promote a controlled drug

release simultaneously to their decomposition [36]. Therefore, the system maintains the release of antibiotics at the target area over a certain period of time, which correlates with the period of decay of the carrier. In this way, possible bacterial infections could be prevented. The drug release kinetics was studied using gentamicin as a model drug. The cumulative gentamicin release curve obtained for the antibacterial coating is reported in Fig. 7.

As reported by Zhang et al. [47], the drug release of nanohybrids is driven by a diffusion-controlled mechanism, in which the radial gentamicin concentration inside the particle causes a gradient and hence becomes the driving force for its own release. Subsequently, the release is affected by the decay of the SiO_2 carrier. In the context of the developed coatings in this project, the discharge of the antibacterial agent (which is incorporated in SiO_2 carriers) is considered to proceed in three steps. Accordingly, an initial burst release within the first day should be followed by a slower release rate in the next days. Then, the limit of overall drug release should be attained with the total degradation of the coating [41,67]. During the initial 24 h, the drug release follows a diffusion mechanism, which is based on a direct proportionality to the concentration gradient of gentamicin that is incorporated in the silica carriers. The kinetics of release is supported by a combination of progressive degradation/decomposition (referring to both the coating and silica particle) and diffusion mechanisms [36,41,67]. Therefore, almost 75% of drug release was achieved for both coating systems after eight days. Finally, after this time point, a very slow drug release is observable, which relates to the already extensive degradation of the chitosan/gelatin matrix.

By direct contact to agar medium, the inhibition capability of the produced coatings to different gram-bacteria was investigated (Fig. 8). The zones of antibacterial activity against gram-positive (*Staphylococcus aureus*) and gram-negative (*Escherichia coli*) bacteria were determined by using the image processing software ImageJ. The following results showed that the bacterial activity of both strains is counteracted by the chitosan/gelatin/Si–Ge nanoparticle coatings on titanium substrates. In comparison with the large inhibition area created for gram (+) and

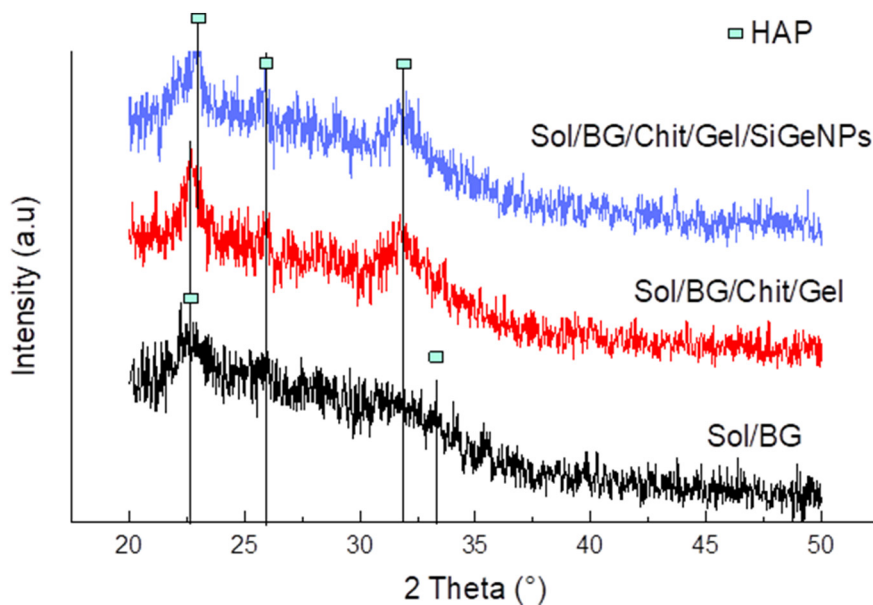


Fig. 6. XRD spectra of dual coatings after SBF immersion for 14 days. The relevant peaks are discussed in the text.

for gram (–) bacteria (8.13 cm² and 13.67 cm², respectively), both the bare Ti samples and the coatings with chitosan/gelatin matrix did not successfully inhibit of bacterial growth, even if, as reported in the literature, chitosan might possess antibacterial properties [40,70]. The low concentration (0.5 g/L) of chitosan in the coatings might play a role in the results.

Turbidity measurements were carried out as an indirect method to analyze the antibacterial effect of the fabricated coatings. Due to the release of gentamicin and its counteraction capability in a bacterial suspension, changes in optical density of the bacteria suspension occur, which were determined at different time points (Fig. 9).

Starting at a bacteria concentration of 0.015 OD_{600nm}, the bacterial growth of both strains was impaired, which is likely through the release of gentamicin from the coated samples. Such coatings are effective against gram-negative (*E.coli*) as well as against gram-positive (*S. aureus*) bacteria. The measured concentration of *Staphylococcus aureus* in the chitosan/gelatin/Si–Ge nanoparticles coating sample was nearly constant during the period of 25 h, slightly different from *Escherichia*

coli concentration, which was constant for 8 h of incubation.

For gram-negative bacteria, there is also an increase in bacterial growth after 10 h of incubation, but this is later followed by a decrease of growth. In general, the results of the turbidity test support and confirm that the coated system exhibits antibacterial properties at the early stages of bacterial growth. Since the incubation of all samples was over a period of one day, these results are also in agreement with the results of the drug release tests and support the spectrometrically determined initial release of around 40% of gentamicin within 24 h.

3.5. Cell biology characterization

The cell viability was measured by using the WST-8 assay after 1 day and 7 days for all coatings. It is noticeable that the four groups of analyzed samples (bare CP-Ti, sol-gel BG drops on CP-Ti, chitosan/gelatin coated CP-Ti and chitosan/gelatin/Si–Ge nanoparticles coated CP-Ti) support the proliferation of bone marrow-derived murine stromal cells (ST-2 cells) (Fig. 10) after 7 days of incubation. As expected, the

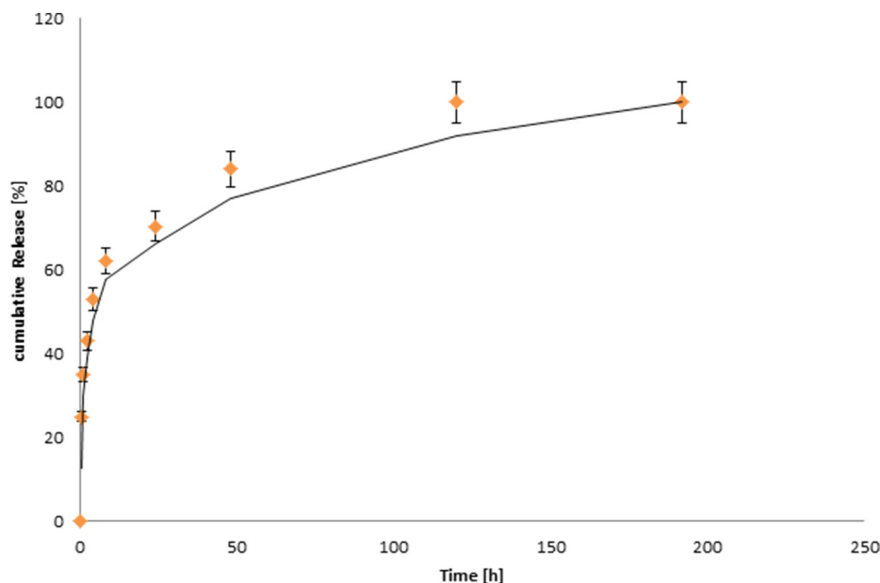


Fig. 7. Cumulative release plot vs time for the dual coatings of titanium substrates after immersion in PBS. The tests were done in triplicate.

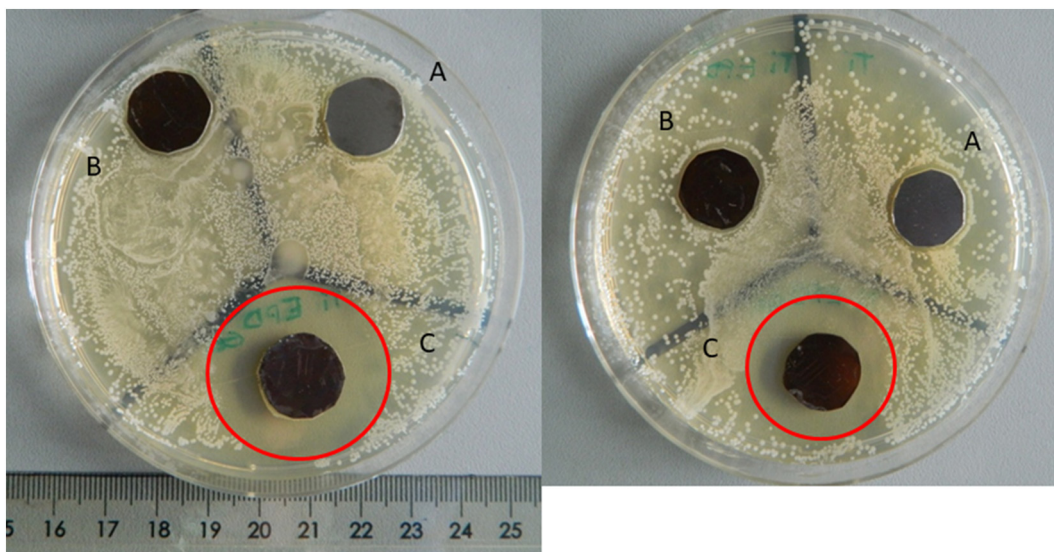


Fig. 8. Antibacterial inhibition halo tests for Ti (A), Ti-EPD coating (B) and Ti EPD coating with SiGe samples (C). (Left) gram (-), (Right) gram (+) bacteria.

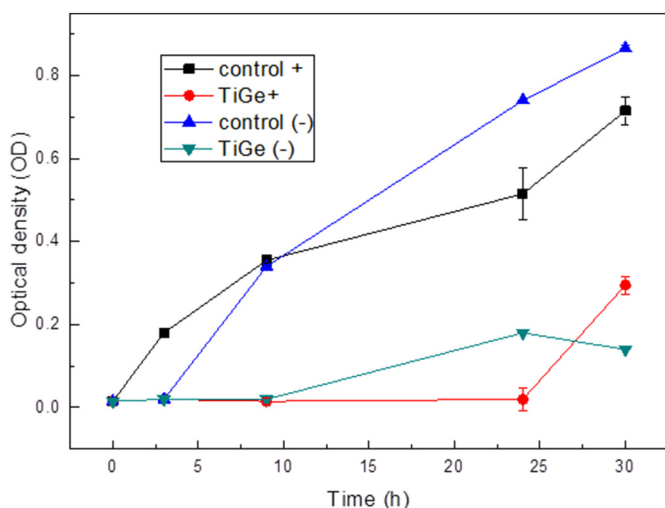


Fig. 9. Optical density with SD of bacteria measured vs time for the EPD-SiGe (called TiGe) coatings and the bare Ti (called control), both gram (-) and (+) bacteria. The tests were performed three times for each condition and each time-point.

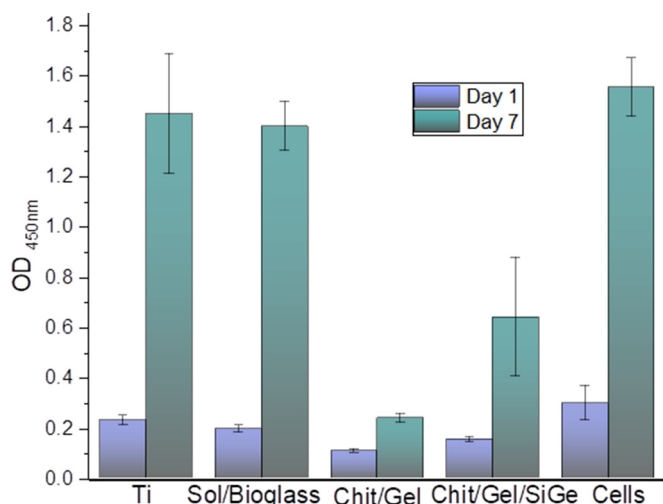


Fig. 10. Cell viability after 1 day (blue) and 7 days (green) for CP-Ti coated samples. Cells seeded in the well without sample were used as control. (For interpretation of the references to color in this figure legend, the reader is referred to the web version of this article.)

presence of silica-based glasses and coatings with amorphous silica on their compositions enhanced cell viability [71–73]. In addition to the spray-deposited BG on CP-Ti samples, the bare CP-Ti seems to promote growth and proliferation of cells for the two time periods measured. It is known that the oxide-layer on titanium has a beneficial influence on cell adhesion [74], what is thought to occur in the bare titanium samples studied here. Also the topography created by polishing the surface generates and promotes cell adhesion and later proliferation [75]. The deposition of BG was done with the aim of extending the bioactive effect of the system for longer periods of time, considering the porous degradable organic layer deposited on top, which was shown to be partially degraded after 7 days.

The results regarding surface roughness showed that the highly rough samples (bare and sprayed titanium) could enable the same rate of cell activity on the first day, which was provided by the chitosan/gelatin matrix on titanium only after seven days. The smooth and even surface topology of chitosan/gelatin films without SiGe nanoparticles might have affected cell adhesion and proliferation at both times analyzed. In fact, both polymers are known for their beneficial properties

regarding cell attachment. In particular, gelatin contains distinct amino acids such as glycine, which can modulate cell adhesion [76]. Since the mobility of chitosan is higher than that of the gelatin during the deposition, the amount of deposited gelatin might be lower or covered by chitosan, so that amino acids, which should promote cell adhesion, are only partially available [77]. The degradation behavior of the coating might also be a reason for this low proliferation rate of cells.

Unlike the WST-8 assay, fluorescence microscopy images of the cell attachment and proliferation (Fig. 11) show that cells were well attached to the chitosan/gelatin films and could proliferate in the given incubation period of 7 days, as shown by Ma et al. [78] and Jiang et al. [77]. The distribution of the adherent cells on the coatings could be evaluated by fluorescence microscopy, which showed that the cell nuclei, stained in blue, were homogeneously dispersed, as reported in Fig. 11. Additionally, the SEM images of the same samples illustrate the wide-spread and proliferated ST-2 cells on the coated substrates (Fig. 12). Based on the fluorescence microscopy observations, it can be stated that cell attachment and proliferation on the coating surfaces occurred in a period of 7 days, possibly without hindrance. On the first

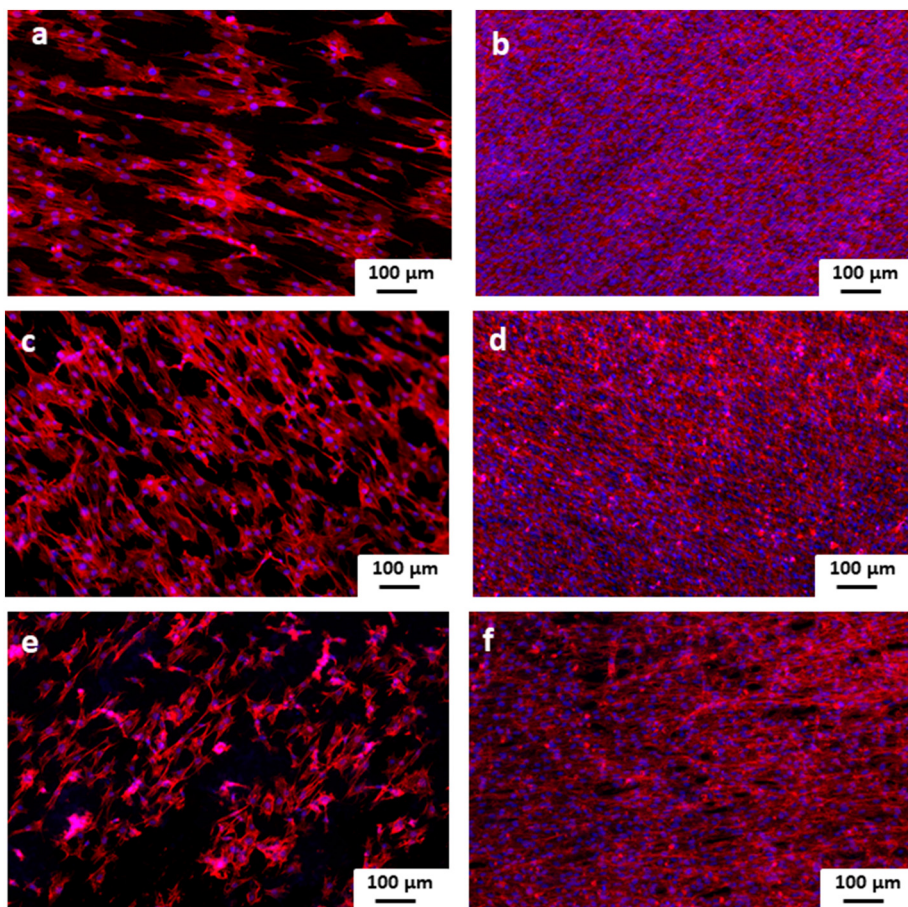


Fig. 11. Fluorescence microscopy images of the CP-Ti samples after 1 and 7 days of cell culture with SP-2 cells. (a) bare CP-Ti, 1 day; (b) bare CP-Ti, 7 days; (c) CP-Ti sprayed BG, 1 day; (d) CP-Ti sprayed BG, 7 days; (e) CP-Ti dual spray EPD coating with SiGe NPs, 1 day; (f) CP-Ti dual-spray EPD coating with SiGe NPs, 7 days. Blue is the nucleus (DAPI staining); red the actin cytoskeleton (Phalloidin). (For interpretation of the references to color in this figure legend, the reader is referred to the web version of this article.)

day of attachment, more elongated cells are frequent, following the polished roughness of the substrate [79], as also observed in Fig. 12(a), (c) and (e). Once settled on the rough surface, the cells grew during 7 days by wide spreading over large areas. As the morphological, physical, and chemical properties of the implant surfaces play a decisive role in cell adhesion and proliferation, all these features have to be taken into account when bioactivity of an implant is analyzed [80]. In this case, the surface roughness of CP-Ti samples, BG and silica coatings bioactivity, chitosan-gelatin chemistry and the generated hydrophilicity of the EPD coatings, are a suitable environment for cellular activity.

The use of silica-loaded nanoparticles in health care applications is becoming increasingly popular [81] due to their versatility and

potential benefits. Pishbin et al. [67] reported the non-toxicity effect of gentamicin towards osteoblast-like human osteosarcoma cells (MG-63), and Mosselhy et al. [82] reported recently that the mortality rate of Zebra fish embryos exposed to silica-gentamicin nanohybrids did not increase. The present results show that no toxicity is generated by the Ti-coated samples, with and without Si-Ge nanoparticles; there is even an enhancement of cell response in terms of attachment and proliferation in the samples with chitosan/gelatin and SiGe nanoparticles, compared with the coatings containing only chitosan and gelatin. Nevertheless, more investigations are needed to evaluate potential adverse effects related to long-term gentamicin release on cell adhesion and proliferation, and to assess silica-gentamicin nanoparticle

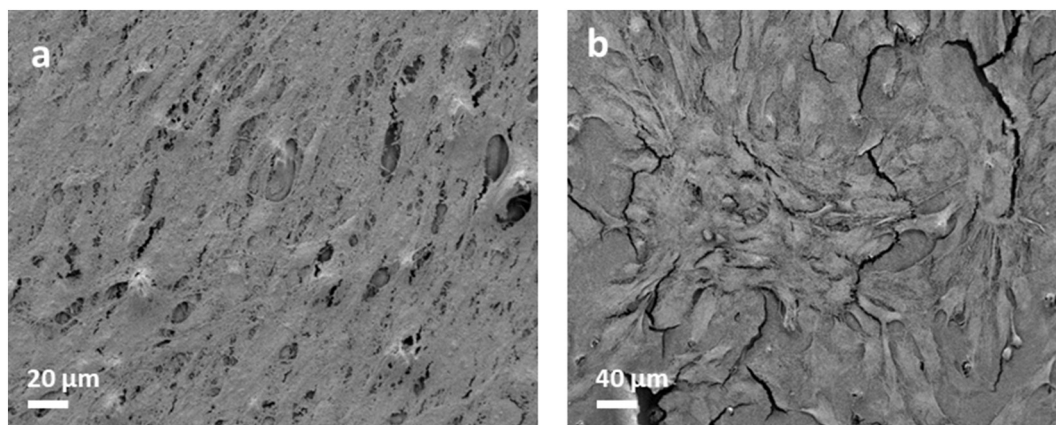


Fig. 12. Scanning Electron Microscopy images of the CP-Ti coated samples after 7 days of cell culture with SP-2 cells. (a) CP-Ti sprayed BG; (b) CP-Ti dual spray EPD coating with SiGe NPs.

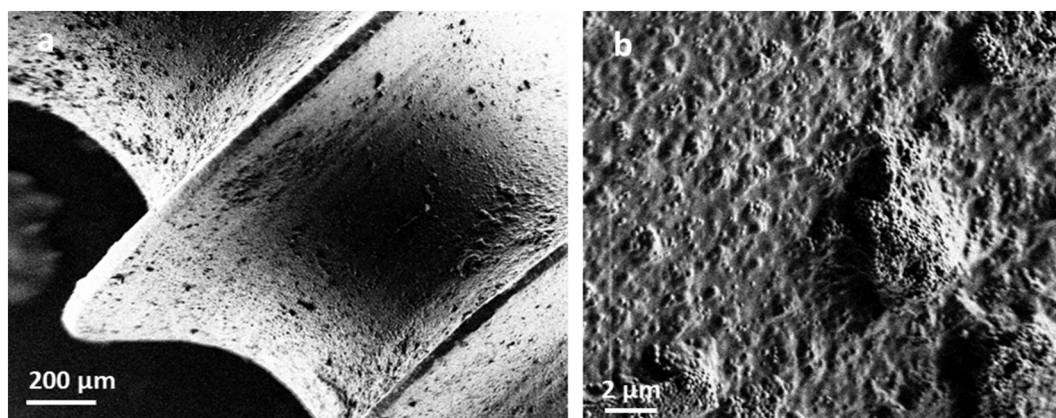


Fig. 13. Scanning Electron Microscopy images of the CP-Ti screws coated with the bilayer system: sol-gel BG spray drops and EPD chitosan/gelatin/SiGe nanoparticles. (a) 138 \times and (b) 1000 \times magnification.

migration over longer periods of time, as well as the mechanism of drug release and silica release.

To illustrate the simple and versatile approach introduced in this study, surgical dental screws were functionalized with the bilayer system. Fig. 13 shows 14 mm length titanium dental screws coated with silica-based sol-gel and BG particles incorporating a chitosan/gelatin/SiGe nanoparticle second layer by EPD. The same coating techniques were applied to obtain a uniform system, noticing the homogeneous distribution of SiGe nanoparticles over the surface.

4. Conclusions

This work presented a new coating approach for the prevention of implant-associated infections involving a biodegradable drug-delivery nanoparticulate system combined with high bioactivity components to induce osseointegration. The simple and versatile coating technique is based on two cost-effective and scalable coating procedures (spraying and electrophoretic deposition) that can be applied to planar and non-symmetric geometries (e.g. surgical screws). The sol-gel sprayed BG layer combined with electrophoretic deposited chitosan/gelatin/SiGe nanoparticles presents a suitable approach to generate bioactive and antibacterial surfaces. Further investigations are needed to evaluate potential adverse long-term effects related to gentamicin release on cell adhesion and proliferation.

Declaration of competing interest

The authors declare that they have no known competing financial interests or personal relationships that could have appeared to influence the work reported in this paper.

Acknowledgments

The authors would like to acknowledge Dr. Agata Lapa for the support with the antibacterial tests, and Prof. Goldmann to DFG (Deutsche Forschungsgemeinschaft, Go598). Dr. Ballarre would like to thank the Alexander von Humboldt Foundation for the Georg Forster Fellowship awarded to experienced researchers.

References

- [1] N.C. Tejwani, I. Immerman, Myths and legends in orthopaedic practice: are we all guilty? *Clin. Orthop. Relat. Res.* 466 (2008) 2861–2872.
- [2] J.S. Hayes, R.G. Richards, The use of titanium and stainless steel in fracture fixation, *Expert Rev Med Devices* 7 (2010) 843–853.
- [3] M. Navarro, A. Michiardi, O. Castano, J.A. Planell, Biomaterials in orthopaedics, *J. R. Soc. Interface* 5 (2008) 1137–1158.
- [4] R.O. Darouiche, Device-associated infections: a macroproblem that starts with microadherence, *Clin. Infect. Dis.* 33 (2001) 1567–1572.
- [5] M. Diefenbeck, T. Mückley, G.O. Hofmann, Prophylaxis and treatment of implant-related infections by local application of antibiotics, *Injury* 37 (2006) S95–S104.
- [6] K. Prasad, O. Bazaka, M. Chua, M. Rochford, L. Fedrick, J. Spoor, R. Symes, M. Tieppo, C. Collins, A. Cao, D. Markwell, K.K. Ostrikov, K. Bazaka, *Metallic biomaterials: current challenges and opportunities*, *Materials (Basel)* 10 (2017).
- [7] Q. Chen, G.A. Thouas, *Metallic implant biomaterials*, *Mater. Sci. Eng. R* 87 (2015) 1–57.
- [8] M. Saini, Y. Singh, P. Arora, V. Arora, K. Jain, *Implant biomaterials: a comprehensive review*, *World Journal of Clinical Cases* 3 (2015) 52–57.
- [9] T. Hanawa, *Research and development of metals for medical devices based on clinical needs*, *Sci. Technol. Adv. Mater.* 13 (2012).
- [10] M. Pennington, R. Grieve, J.S. Sekhon, P. Gregg, N. Black, J.H. van der Meulen, Cemented, cementless, and hybrid prostheses for total hip replacement: cost effectiveness analysis, *BMJ* 346 (2013).
- [11] R.H. ROTHMAN, J.C. COHN, Cemented versus cementless total hip arthroplasty: a critical review, *Clin. Orthop. Relat. Res.* 254 (1990) 153–169.
- [12] D.M.D. Ehrenfest, P.G. Coelho, K. Byung-Soo, Y.T. Sul, T. Albrektsson, Classification of osseointegrated implant surfaces: materials, chemistry and topography, *Trends Biotechnol.* 28 (2009) 198–206.
- [13] T. Albrektsson, P.I. Branemark, H.A. Hansson, J. Lindstrom, Osseointegrated titanium implants. Requirements for ensuring a long-lasting, direct bone-to-implant anchorage in man, *Acta Orthop. Scand.* 52 (1981) 155–170.
- [14] C.J. Brinker, A.J. Hurd, P.R. Schunk, G.C. Frye, C.S. Ashley, Review of sol-gel thin film formation, *J. Non-Cryst. Solids* 147–148 (1992) 424–436.
- [15] M. Guglielmi, Rivestimenti sottili mediante dip coating con metodo sol-gel, *Revista della Staz. Sper.* 4 (1988) 197–199.
- [16] S. Sanchez, M. In, Molecular design of alkoxide precursors for the synthesis of hybrid organic-inorganic gels, *J. Non-Cryst. Solids* 147–148 (1992) 1–12.
- [17] O. de Sanctis, L. Gomez, N. Pellegrini, C. Parodi, A. Marajofsky, A. Duran, Protective glass coatings on metallic substrates, *J. Non-Cryst. Solids* 121 (1990) 338–343.
- [18] L. Pawlowski, *The Science and Engineering of Thermal Spray Coatings*, second edition, (2008).
- [19] S. Omar, S. Pellice, J. Ballarre, S. Ceré, Hybrid organic-inorganic silica-based coatings deposited by spray technique, *Procedia Mater. Sci.* 9 (2015) 469–476.
- [20] D. Wang, P. Bierwagen Gordon, Sol-gel coatings on metals for corrosion protection, *Progress in Organic Coatings* 64 (2009) 327–338.
- [21] S.A. Omar, J. Ballarre, S.M. Ceré, Protection and functionalization of AISI 316 L stainless steel for orthopedic implants: hybrid coating and sol gel glasses by spray to promote bioactivity, *Electrochim. Acta* 203 (2016) 309–315.
- [22] F. Bairo, C. Vitale-Brovarone, Feasibility of glass-ceramic coatings on alumina prosthetic implants by airbrush spraying method, *Ceram. Int.* 41 (2015) 2150–2159.
- [23] V. Krishnan, T. Lakshmi, Bioglass: a novel biocompatible innovation, *Journal of Advanced Pharmaceutical Technology & Research* 4 (2013) 78–83.
- [24] L.L. Hench, H.A. Paschall, Direct chemical bond of bioactive glass ceramic materials to bone and muscle, *J. Biomed. Mater. Res.* 7 (1973) 25–42.
- [25] J.R. Jones, Review of bioactive glass: from Hench to hybrids, *Acta Biomater.* 9 (2013) 4457–4486.
- [26] L.L. Hench, Opening paper 2015- some comments on bioglass: four eras of discovery and development, *Biomedical Glasses* 1 (2015) 1–11.
- [27] S. Ahn, S. Lee, J. Kook, B. Lim, Experimental antimicrobial orthodontic adhesives using nanofillers and silver nanoparticles, *Dent. Mater.* 25 (2009) 206–213.
- [28] L. Li, L. Wang, Y. Xu, L. Lv, Preparation of gentamicin-loaded electrospray coating on titanium implants and a study of their properties in vitro, *Arch. Orthop. Trauma Surg.* 132 (2012) 897–903.
- [29] K. Subramani, R.T. Mathew, Titanium surface modification techniques for dental implants-from microscale to nanoscale, *Emerging Nanotechnologies in Dentistry*, 2012, pp. 85–102.
- [30] L. Zhang, J. Yan, Z. Yin, C. Tang, Y. Guo, D. Li, B. Wei, Y. Xu, Q. Gu, L. Wang, Electrospun vancomycin-loaded coating on titanium implants for the prevention of implant-associated infections, *Int. J. Nanomedicine* 9 (2014) 3027–3036.

- [31] H. Qin, Y. Zhao, Z. An, M. Cheng, Q. Wang, T. Cheng, Q. Wang, J. Wang, Y. Jiang, X. Zhang, G. Yuan, Enhanced antibacterial properties, biocompatibility, and corrosion resistance of degradable Mg-Nd-Zn-Zr alloy, *Biomaterials* 53 (2015) 211–220.
- [32] J. Wang, G. Wu, X. Liu, G. Sun, D. Li, H. Wei, A decomposable silica-based antibacterial coating for percutaneous titanium implant, *Int. J. Nanomedicine* 12 (2017) 371–379.
- [33] R.D. Moore, P.S. Lietman, C.R. Smith, Clinical response to aminoglycoside therapy: importance of the ratio of peak concentration to minimal inhibitory concentration, *J. Infect. Dis.* 155 (1987) 93–99.
- [34] P. Ducheyne, K. Healy, D.W. Huttmacher, D. Grainger, C. James, *Comprehensive Biomaterials*, Elsevier Science, 2015.
- [35] I.-Y. Kim, E. Joachim, H. Choi, K. Kim, Toxicity of silica nanoparticles depends on size, dose, and cell type, *Nanomedicine* 11 (2015) 1407–1416.
- [36] S. Zhang, Z. Chu, C. Yin, C. Zhang, G. Lin, Q. Li, Controllable drug release and simultaneously carrier decomposition of SiO₂-drug composite nanoparticles, *J. Am. Chem. Soc.* 135 (2013) 5709–5716.
- [37] L. Besra, M. Liu, A review on fundamentals and applications of electrophoretic deposition (EPD), *Prog. Mater. Sci.* 52 (2007) 1–61.
- [38] A.R. Boccaccini, J. Cho, T. Subhani, C. Kaya, F. Kaya, Electrophoretic deposition of carbon nanotube-ceramic nanocomposites, *J. Eur. Ceram. Soc.* 30 (2010) 1115–1129.
- [39] F. Pishbin, V. Mourinho, J.B. Gilchrist, D.W. McComb, S. Kreppel, V. Salih, M.P. Ryan, A.R. Boccaccini, Single-step electrochemical deposition of antimicrobial orthopaedic coatings based on a bioactive glass/chitosan/nano-silver composite system, *Acta Biomater.* 9 (2013) 7469–7479.
- [40] A.R. Boccaccini, S. Keim, R. Ma, Y. Li, I. Zhitomirsky, Electrophoretic deposition of biomaterials, *J. R. Soc. Interface* 7 (Suppl. 5) (2010) S581–S613.
- [41] J. Song, Q. Chen, Y. Zhang, M. Diba, E. Kolwijck, J. Shao, J.A. Jansen, F. Yang, A.R. Boccaccini, S.C.G. Leuvenburgh, Electrophoretic deposition of chitosan coatings modified with gelatin nanospheres to tune the release of antibiotics, *ACS Appl. Mater. Interfaces* 8 (2016) 13785–13792.
- [42] B. Ferrari, R. Moreno, EPD kinetics: a review, *J. Eur. Ceram. Soc.* 30 (2010) 1069–1078.
- [43] I. Corni, M.P. Ryan, A.R. Boccaccini, Electrophoretic deposition: from traditional ceramics to nanotechnology, *J. Eur. Ceram. Soc.* 28 (2008) 1353–1367.
- [44] F. Pishbin, A. Simchi, M.P. Ryan, A.R. Boccaccini, Electrophoretic deposition of chitosan/45S5 Bioglass® composite coatings for orthopaedic applications, *Surf. Coat. Technol.* 205 (2011) 5260–5268.
- [45] F. Gebhardt, S. Seuss, M.C. Turhan, H. Hornberger, S. Virtanen, A.R. Boccaccini, Characterization of electrophoretic chitosan coatings on stainless steel, *Mater. Lett.* 66 (2012) 302–304.
- [46] K.D. Patel, R.K. Singh, E.J. Lee, C.M. Han, J.E. Won, J.C. Knowles, H.W. Kim, Tailoring solubility and drug release from electrophoretic deposited chitosan-gelatin films on titanium, *Surf. Coat. Technol.* 242 (2014) 232–236.
- [47] Z. Zhang, X. Cheng, Y. Yao, J. Luo, Q. Tang, H. Wu, S. Lin, C. Han, Q. Wei, L. Chen, Electrophoretic deposition of chitosan/gelatin coatings with controlled porous surface topography to enhance initial osteoblast adhesive responses, *J. Mater. Chem. B* 4 (2016) 7584–7595.
- [48] M. Dash, F. Chiellini, R.M. Ontenbrite, E. Chiellini, Chitosan - a versatile semi-synthetic polymer in biomedical applications, *Progress in Polymer Science (Oxford)* 36 (2011) 981–1014.
- [49] M. Höhlinger, S. Heise, V. Wagener, A.R. Boccaccini, S. Virtanen, Developing surface pre-treatments for electrophoretic deposition of biofunctional chitosan-bioactive glass coatings on a WE43 magnesium alloy, *Appl. Surf. Sci.* 405 (2017) 441–448.
- [50] T. Kokubo, H. Kushitani, C. Ohtsuki, S. Sakka, Chemical reaction of bioactive glass and glass - ceramics with a simulated body fluid, *J. Mater. Sci. Mater. M* 3 (1992) 79–83.
- [51] T. Kokubo, H. Kushitani, S. Sakka, T. Kitsugi, T. Yamamuro, Solutions able to produce in vivo surface - structure changes in bioactive glass - ceramic A. W. J. *Biomed. Mater. Res.* 24 (1990) 721–734.
- [52] T. Kokubo, H. Takadama, How useful is SBF in predicting in vivo bone bioactivity? *Biomaterials* 27 (2006) 2907–2915.
- [53] P. Frutos, S. Torrado, M.E. Perez-Lorenzo, G. Frutos, A validated quantitative colorimetric assay for gentamicin, *J. Pharm. Biomed. Anal.* 21 (2000) 1149–1159.
- [54] C.A. Schneider, W.S. Rasband, K.W. Eliceiri, NIH Image to ImageJ: 25 years of image analysis, *Nat. Methods* 9 (2012) 671–675.
- [55] A.M. Mebert, C. Aimé, G.S. Alvarez, Y. Shi, S.A. Flor, S.E. Lucangiolli, M.F. Desimone, T. Coradin, Silica core-shell particles for the dual delivery of gentamicin and rifamycin antibiotics, *J. Mater. Chem. B* 4 (2016) 3135–3144.
- [56] N.G. Voron'ko, S.R. Derkach, Y.A. Kuchina, N.I. Sokolan, The chitosan-gelatin (bio) polyelectrolyte complexes formation in an acidic medium, *Carbohydr. Polym.* 138 (2016) 265–272.
- [57] S. Seuss, A.R. Boccaccini, Electrophoretic deposition of biological macromolecules, drugs, and cells, *Biomacromolecules* 14 (2013) 3355–3369.
- [58] A.S. Dukhin, P.J. Goetz, Characterization of Liquids, Dispersions, Emulsions, and Porous Materials Using Ultrasound, (2017).
- [59] K.L. Menzies, L. Jones, The impact of contact angle on the biocompatibility of biomaterials, *Optom. Vis. Sci.* 87 (2010) 387–399.
- [60] J.H. Lee, G. Khang, J.W. Lee, H.B. Lee, Interaction of different types of cells on polymer surfaces with wettability gradient, *J. Colloid Interface Sci.* 205 (1998) 323–330.
- [61] J.D. Bumgardner, R. Wiser, S.H. Elder, R. Jouett, Y. Yang, J.L. Ong, Contact angle, protein adsorption and osteoblast precursor cell attachment to chitosan coatings bonded to titanium, *J. Biomater. Sci. Polym. Ed.* 14 (2003) 1401–1409.
- [62] V. Mittal, *Nanocomposites With Biodegradable Polymers: Synthesis, Properties, and Future Perspectives*, (2011).
- [63] B.L. Pereira, P. Tummler, C.E.B. Marino, P.C. Soares, N.K. Kuromoto, Titanium bioactivity surfaces obtained by chemical/electrochemical treatments, *Revista Materia* 19 (2014) 16–23.
- [64] L. Ghasemi-Mobarakeh, M.P. Prabhakaran, M. Morshed, M.H. Nasr-Esfahani, S. Ramakrishna, Electrospun poly(ϵ -caprolactone)/gelatin nanofibrous scaffolds for nerve tissue engineering, *Biomaterials* 29 (2008) 4532–4539.
- [65] R. Murugan, S. Ramakrishna, Bioresorbable composite bone paste using polysaccharide based nano hydroxyapatite, *Biomaterials* 25 (2004) 3829–3835.
- [66] M. Cerruti, D. Greenspan, K. Powers, Effect of pH and ionic strength on the reactivity of Bioglass® 45S5, *Biomaterials* 26 (2005) 1665–1674.
- [67] F. Pishbin, V. Mourinho, S. Flor, S. Kreppel, V. Salih, M.P. Ryan, A.R. Boccaccini, Electrophoretic deposition of gentamicin-loaded bioactive glass/chitosan composite coatings for orthopaedic implants, *ACS Appl. Mater. Interfaces* 6 (2014) 8796–8806.
- [68] A. Stoch, W. Jastrzębski, A. Brożek, B. Trybalska, M. Cichocińska, E. Szarawara, FTIR monitoring of the growth of the carbonate containing apatite layers from simulated and natural body fluids, *J. Mol. Struct.* 511–512 (1999) 287–294.
- [69] S. Kumar, J. Koh, Physicochemical, optical and biological activity of chitosan-chromone derivative for biomedical applications, *Int. J. Mol. Sci.* 13 (2012) 6103–6116.
- [70] C.K.S. Pillai, W. Paul, C.P. Sharma, Chitin and chitosan polymers: chemistry, solubility and fiber formation, *Progress in Polymer Science (Oxford)* 34 (2009) 641–678.
- [71] P. Ducheyne, Q. Qiu, Bioactive ceramics: the effect of surface reactivity on bone formation and bone cell function, *Biomaterials* 20 (1999) 2287–2303.
- [72] S.K. Misra, T. Ansari, D. Mohn, S.P. Valappil, T.J. Brunner, W.J. Stark, I. Roy, J.C. Knowles, P.D. Sibbons, E.V. Jones, A.R. Boccaccini, V. Salih, Effect of nanoparticulate bioactive glass particles on bioactivity and cytocompatibility of poly(3-hydroxybutyrate) composites, *J. R. Soc. Interface* 7 (2010) 453–465.
- [73] S. Areva, V. Ääritalo, S. Tuusa, M. Jokinen, M. Lindén, T. Peltola, Sol-Gel-derived TiO₂-SiO₂ implant coatings for direct tissue attachment. Part II: evaluation of cell response, *J. Mater. Sci. Mater. Med.* 18 (2007) 1633–1642.
- [74] R.K. Sinha, F. Morris, S.A. Shah, R.S. Tuan, Surface composition of orthopaedic implant metals regulates cell attachment, spreading, and cytoskeletal organization of primary human osteoblasts in vitro, *Clin. Orthop. Relat. Res.* (1994) 258–272.
- [75] L. Ponsonnet, K. Reybier, N. Jaffrezic, V. Comte, C. Lagneau, M. Lissac, C. Martelet, Relationship between surface properties (roughness, wettability) of titanium and titanium alloys and cell behaviour, *Mater. Sci. Eng. C* 23 (2003) 551–560.
- [76] R. Pankov, K.M. Yamada, Fibronectin at a glance, *J. Cell Sci.* 115 (2002) 3861–3863.
- [77] T. Jiang, Z. Zhang, Y. Zhou, Y. Liu, Z. Wang, H. Tong, X. Shen, Y. Wang, Surface functionalization of titanium with chitosan/gelatin via electrophoretic deposition: characterization and cell behavior, *Biomacromolecules* 11 (2010) 1254–1260.
- [78] K. Ma, X. Cai, Y. Zhou, Z. Zhang, T. Jiang, Y. Wang, Osteogenic property of a biodegradable three-dimensional macroporous hydrogel coating on titanium implants fabricated via EPD, *Biomaterials (Bristol)* 9 (2014).
- [79] K. Anselme, M. Bigerelle, B. Noel, E. Dufresne, D. Judas, A. Iost, P. Hardouin, Qualitative and quantitative study of human osteoblast adhesion on materials with various surface roughnesses, *J. Biomed. Mater. Res.* 49 (2000) 155–166.
- [80] D.A. Puleo, A. Nanci, Understanding and controlling the bone-implant interface, *Biomaterials* 20 (1999) 2311–2321.
- [81] A.M. Mebert, C.J. Baglolo, M.F. Desimone, D. Maysinger, Nanoengineered silica: properties, applications and toxicity, *Food Chem. Toxicol.* 109 (2017) 753–770.
- [82] D.A. Mosselhy, W. He, U. Hynönen, Y. Meng, P. Mohammadi, A. Palva, Q. Feng, S.P. Hannula, K. Nordström, M.B. Linder, Silica-gentamicin nanohybrids: combating antibiotic resistance, bacterial biofilms, and in vivo toxicity, *Int. J. Nanomedicine* 13 (2018) 7939–7957.